Transactions on Modelling and Simulation vol 22, © 1999 WIT Press, www.witpress.com, ISSN 1743-355X

Investigating ICCP system design of ship with waterjet propulsion using boundary element technology

Pei Yuan Hang
DSO National Laboratories, Singapore 118230

Abstract

This paper presents an approach to design the impressed corrosion cathodic protection (ICCP) system integrating complicated ship hull and internal structures of waterjet using boundary element technology. Design optimization of anode numbers and locations is determined based on the detailed boundary element analysis and penalty method. Considering the changes of boundary conditions, the corrosion protection is evaluated while ship is travelling at different speeds and paint status.

1 Introduction

Waterjet is often chosen for ships operating in waters with restricted depths as it presents a solution with minimum draught and protected propulsor. The basic components of a waterjet unit are illustrated in figure 1. They are the inlet, the pump unit consisting of shaft, impellers, water box and impeller ring, and nozzle. The action of the pump causes the water to pass through the system. The pump adds energy to the water, which is converted in the outlet nozzle in an increase of momentum of the flow [1].

Cathodic protection has been widely used in corrosion protection. The design of the cathodic protection system, either anode cathodic protection(CP) or impressed current cathodic protection (ICCP) system, Laplace's and Poission's equation must be solved with the relevant boundary conditions to give the current and potential distribution in the solution domain.

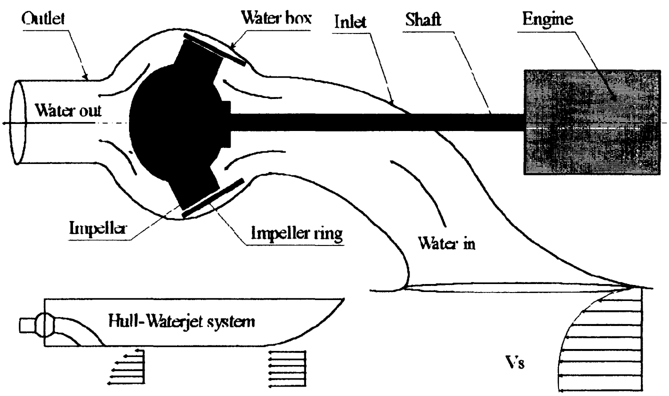

Figure 1: Waterjet structure scheme

The solution to the equations, even for relatively simple geometry, analytical solutions are usually not possible. Various numerical approaches have therefore been adopted. Boundary element method is a proficient numerical method that suits for the modelling of ship's cathodic protection system [2-8, 13].

The present work approachs the ICCP system design of ship with waterjet propulsion considering its complex structure using boundary element technology. The design process achieved an optimum location of anodes and reference electrodes to protect the ship hull and waterjet structures from corrosion effectively and sufficiently.

2 The boundary element model

The governing equation in the bounded uniform seawater medium is:

$$\nabla \cdot (-\sigma \, \nabla u) = 0 \tag{1}$$

where u is the electropotential, σ is the conductivity. The electric current is directly related to the first derivative of electric potential, u:

$$j = -\sigma \nabla u \tag{2}$$

where j is the electric current density. Boundary condition in the solution domain is defined by:

$$\Gamma = \Gamma_A + \Gamma_C + \Gamma_I \tag{3}$$

where Γ_A is the anodic surface, Γ_C is the cathodic surface and Γ_I is the insulated surface.

Transactions on Modelling and Simulation vol 22, © 1999 WIT Press, www.witpress.com, ISSN 1743-355X

The boundary element formulation in electropotential is well established [6]. The principle advantage of boundary element method is that its result is very accurate and the mesh discretization investigated is only the boundaries of the solution domain. The normal electric potential is directly obtained. The boundary element software BEASY-CP [12] was used in present study.

3 Material polarisation

The material polarisation data describes the electrochemical reaction and the environmental factors and can be generally expresses as [7-9]:

$$j = f(u, h, v, d, t, s, b, etc) \quad (4)$$

where, u is the potential, v is the flow velocity of the electrolyte, d is the depth, t is the temperature, h is the film thickness, s is the salinity and b is the bio-fouling.

In the present design, distinct materials are included. Ship hull, shell of the waterjet including inlet, outlet and water box are made of steel. Painting and coating on the steel surfaces is used to provide the initial avoidance from corrosion. The shaft and impellers of waterjet are made of stainless steel without painting. The impeller ring is made of stainless steel and is only coated on the outer diameter surface.

With such design, there is a significant risk of galvanic corrosion on the steel surface. The corrosion can be accelerated in the materials used in the waterjet by the high water velocity and turbulent flow. The highly turbulence flow of seawater on the surface of impeller and impeller ring can cause pitting, crevice attack, erosion, cavitation damage, and corrosion fatigue. Fouling increases the localised corrosion, which is accelerated as metallic ions leached from anti-fouling paint. As steel surfaces are coated, severe local attack can occur rapidly on any damaged surface due to the very high current density caused by the galvanic action.

Under low velocity of seawater in the waterjet, less available oxygen made its low concentration more important than the rates of oxygen reactions on the different metal surface. With the greater supply of oxygen reaction from seawater moving at the higher velocity the oxygen reduction reaction on the different metal surfaces had a major effect on the extent of galvanic corrosion. The current density to obtain a sufficient protection level depends on the seawater velocity and the degree of turbulence.

The velocity of the seawater flowing in the waterjet depends on the speed of the ship. The thrust T of waterjet system is represented by:

$$T = \rho\, Q\, (V_n - V_s) \quad (5)$$

where Q is the flow rate through the waterjet, V_n and V_s is the averaged water velocity leaving nozzle and enter the inlet respectively.

The headrise produced by the pump is equal to the head needed to be produced by the waterjet and overcome the losses in the inlet and outlet ducting minus the beneficial head of the incoming flow:

$$H = \frac{V_n^2}{2g}(1+\Phi) - \frac{V_s^2}{2g}(1-\epsilon) + h_s \tag{6}$$

where H is the head delivered by pump, Φ is the loss factor of outlet ducting, g is constant of gravity, ϵ is the loss factor of inlet ducting and h_s is the elevation of waterjet.

The required shaft power is a function of speed of vessel and given by:

$$P_s = \frac{\rho\, g\, H\, Q}{\eta_R\, \eta_P} = \frac{R_{BH} V_0}{\eta_{oa}} \tag{7}$$

where P_s is shaft power, R_{BH} is the bare hull resistance, η_R and η_P is relative rotating efficiency and pump efficiency in uniform flow respectively, η_{oa} is the overall efficiency of the waterjet and V_0 is the ship speed.

The effect of hydrodynamic of the seawater flow in the waterjet is determined by a condenser tube which has the mass transfer correlation given for fully developed turbulent flow [10]:

$$Sh = 0.023\, Re^{0.8}\, Sc^{1/3} \tag{8}$$

where Sh is the Sherwood number, R_e is the Reynolds number and Sc is the Schmidt number.

The modification of this correlation is to introduce a friction factor, the Fanning fraction factor [11]:

$$\frac{f}{2} = \frac{\tau_w}{\rho\, v^2} \tag{9}$$

where τ_w is the well shear stress and ρ is the seawater density.

For turbulent flow in smooth pipes the fraction factor has been corrected to the Reynolds numbers [11]:

$$f = 0.316\, Re^{-0.25} \tag{10}$$

Therefore the current in term of turbulent flow in pipes:

$$Sh = 0.073\, f\, Re^{1.05}\, Sc^{1/3} \tag{11}$$

The ambient temperature changes may increase or decrease the current. Literature data [7-9] were used in present computer model. The temperature and oxygen concentration of the seawater is taken as 30° and 6 $[O_2]$mg/l respectively.

Definition of above parameters can be determined either by experiment or by computation. In the present computer model, the velocity of seawater in the waterjet and speed of the shaft is derived from computation results.

Having defined the boundary conditions in the boundary element model, the material polarisation [8, 9] used in the computer model was modified by taking the influence of seawater velocity and temperature. The higher speed of seawater associated with turbulence flow conditions may increase the rate of the electrochemical reaction by more than an order of magnitude beyond that observed for quiescent conditions.

4 Optimization of ICCP system

The design of ICCP system is the crucial process and has significant influences to the corrosion protection on the wetted surface of the ship.

The ship investigated is 55 meters in length and installed two waterjets. The ship hull ICCP system consists of 4 anodes and 2 distributed centre-controlled power supplies. An integrated boundary element model was built including one waterjet and half of ship hull due to the symmetry of the ship construction.

The definition of the paint status, location and damaged area in the computer model is based on the observations of the same and similar class of ships in dry-dock after the ships have served a certain period of time. Paint are damaged on certain regions including parts of the hull and internal surface of waterjet, especially on the aft zone around inlet of the waterjet and internal surface of the waterjet.

To determine the characteristics of the damaged paint, the conductivity of old and new paint was measured and compared. The observed damaged paint status is that there are a lot of small, local bare steel surfaces on the damaged paint surfaces. In the present computer model, the positions of the damaged paint surface and percentage of bare steel surfaces on the damaged paint surface are defined based on the statistics to the observations of the real ships.

The equivalent conductivity on damaged paint surface is derived based on the ratio of bare steel surface and painted surface. The equivalent conductivity of damaged paint surface then is modelled by means of percentage of the polarisation response of steel. The perfect painted steel hull was modelled as insulated surfaces.

The ship operates in the restricted water depth. The boundary element model was set up as a 20 metres flat bottom and surrounding boundaries far from the solution domain interest. The seawater is defined with constant conductivity of 5 S/m in the computer model. The combined boundary element model discretization is either a 9-point quadrilateral or 6-nodes triangular elements and mesh discretization of the ship, which amounts to 1162 elements and 6733 nodes.

Required potential level on the wetted surface of the ship is determined by anode currents and has to be obtained by an iterative process by adjusting anode currents. A typical boundary element solution in the present computer model used 5 hours in the DEC Alpha 500 workstation.

The optimum design goal was set to produce an evenly distributed electric potential on the wetted surface of the ship as well as minimise the power consumption required. The objective function and constrain condition is determined by:

$$min \quad f(i,s,u,P) = \left(\sum_{k=1}^{n} \frac{| u_t |}{| u_t | - | u_t - u_k |} \right) - \frac{\xi}{P(i,u,s)} \tag{12}$$

$$with \quad u_{min} \leq u_k \leq u_{max} \quad k = 1,...,n \tag{13}$$

$$and \quad x_{min} \leq x_m \leq x_{max} \quad m = 1,...,p \tag{14}$$

where, $P(i,u,s)$ is the electric power consumption on the anodes, ξ is a weight factor to measure the power consumption in the objective function, i is the anode electric currents, u is the potential on the measurement points, s is the location of the anodes, u_{min} and u_{max} is the minimum and maximum protection potential level on wetted surface of the ship and set up as -0.78 Volt to -0.88 Volt Ag/AgCl respectively, $u_k = (u_1, u_2, ..., u_n)$ is the potentials on the measurement points which meet the requirement $u_{min} \leq u_k \leq u_{max}$, u_t is the threshold potential and is defined as equals to -0.83 Volt Ag/AgCl on reference cell, $x_m = (x_1, x_2, ...x_p)$ is the measurement points on the wetted surface, usually $p \geq n$. The objective function presents the measurement to the uniformity of the potential distributions on the wetted surface of the ship with a particular anode arrangement.

In the design phase, the paint on the surfaces of shell of the waterjet and outer diameter of the impeller ring was treated as damaged paint surface. 15% paint surface on the ship hull, most concentrating on aft zone around inlet of the waterjet, is defined as damaged paint. The conductivity of above damaged paint surfaces is defined as 10% polarisation response of the steel. The moving components of waterjet and inner diameter of impeller ring are modelled as bare surface.

In the design of the ICCP system, the influence of the individual ICCP systems of ship and waterjet has to be considered. A large amount of electric currents are injected into the wetted surface of the waterjet due to the high turbulence of seawater in the operation. The anode currents of the hull ICCP system have to avoid falling into the trap caused by the high current cathodic cells on the wetted surface inside the waterjet.

The optimization process to the anode numbers and locations was implemented by a computer program based on penalty method [14]. The expended objective function of the algorithm is defined as:

$$\min_{x_l \in D} F(i,s,u,P) = f(i,s,u,P) + r \sum \frac{1}{G(i,s,u,P)} \tag{15}$$

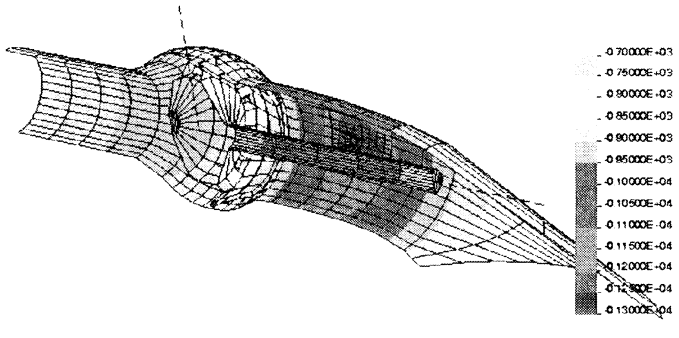

Figure 2: The protection potential (mV) distribution of initial design

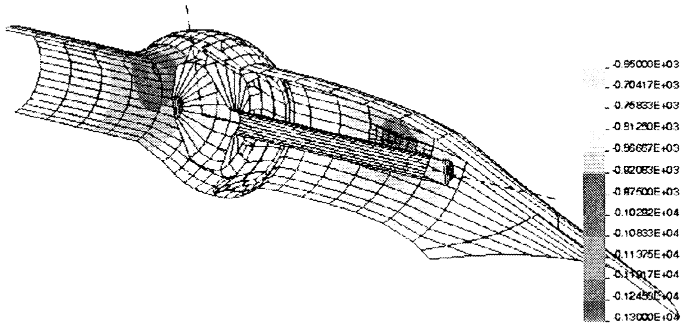

Figure 3: The protection potential (mV) distribution of improved design

where $x_l = x_1, x_2, ..., x_L$ is the anode locations, L is the total numbers of anode and D is the domain of wetted surface of the ship. r is a positive weighting coefficient which ensure that during the optimization the constrains $G(i, s, u, P)$ are not violated. The effect of this function is to create an artificial minimum in the vicinity of the boundary. The constrains is defined to meet following threshold:

$$G(i,s,u,P) = \left(\sum_{k=1}^{n} | u_k | - \sum_{j=1}^{N} | u_j | \right) \geq 0 \tag{16}$$

where the second term of 16 is a defined threshold potential and N is a threshold number of measured potentials which meet $u_{min} \leq u_j \leq u_{max}$, $G(i, s, u, P)$ therefore is an overall measurement to the potential distribution of a particular anode arrangement. The optimization behaviour relays on the choice of weighting coefficient r and the expended constrains. These parameters have been chosen based on the experience during the optimization process.

Transactions on Modelling and Simulation vol 22, © 1999 WIT Press, www.witpress.com, ISSN 1743-355X

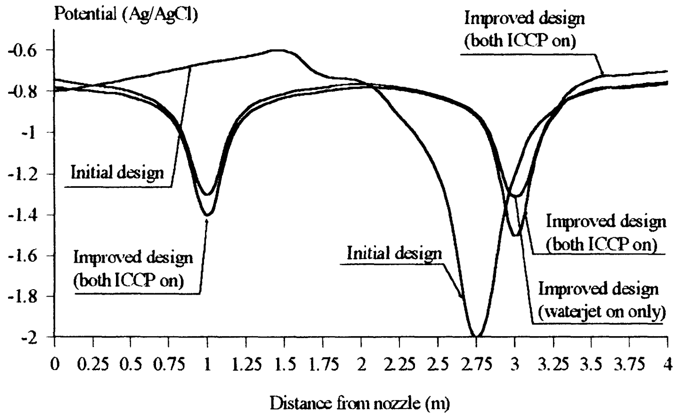

Figure 4: Comparison of potential (V) distribution of different design

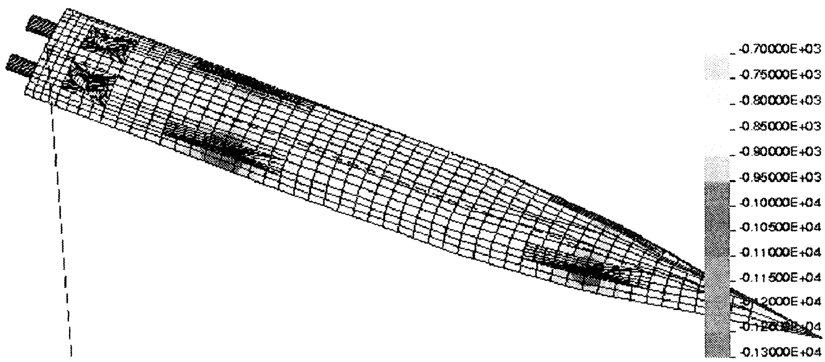

Figure 5: The potential (mV) distribution on ship hull and waterjet

Optimization process was carried out based on (12 - 16) to design the number and location of the anodes of the two individual ICCP systems.

In the preliminary design, the anodes were located on the inlet of the waterjet and a group anode was located on the position between the water box and impeller ring. The potential profile is shown in figure 2 when ship speed is 5 knots. On the nozzle and water box surfaces the potential is kept to below the protection threshold regardless of the anodes were moved to their optimum positions. The narrow area between impeller and impeller ring has the function to block the current to flow through it.

The under protection on the outlet surface has to be solved, as severe corrosion damage may attack the surface. A group of anode therefore was located on the outlet surface to improve the protection on the outlet and

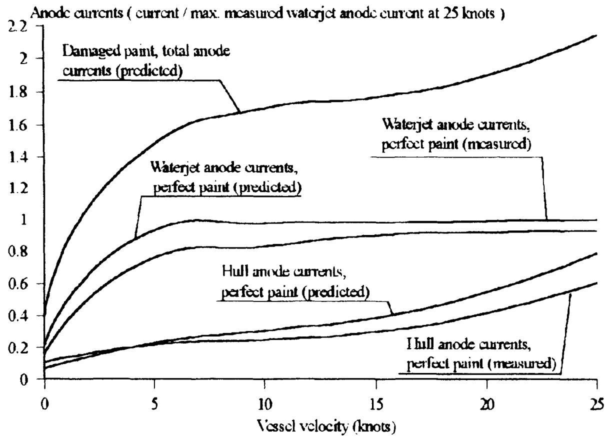

Figure 6: Anode currents in different ship speeds with different paint status

water box surface and reduces the overprotection risk on the inlet surface. An evenly distributed potential was achieved both on the inlet and nozzle surfaces by this design after optimization process as shown in figure 3.

Boundary element modelling provide a precise tool to identify and compare different designs. Figure 4 illustrates the potential distribution along the centre horizontal line on the internal surface of the waterjet from the different designs and the influences between hull and waterjet ICCP systems. The ship speed under investigation is 5 knots.

The optimization design process produces a flat distributed potential over the ship hull surface and internal surface of the waterjet. Taking the influences of ICCP systems on ship hull and waterjet, seawater speed and temperature into account, the achieved potential distribution of the ship and waterjet ICCP system design while ship is travelling in 5 knots is illustrated in figure 5. By observing the potential profile, the reference cells were then located at the position of most representatives to the potential distribution.

Boundary element modelling results are compared with ship's measurement results. The computation is made under the condition that all static surface in the waterjet has the perfect paint, the shaft, inner surface of the impeller ring and impellers have no paint. Small portion of paint on the hull surface, most on the aft zone, is modelled as bare steel surface based on the observation. The influences of seawater velocities on the wetted surface of the ship were considered in the computer model. The anode current when ship is travelling at the different speeds is illustrated in figure 6. Good agreement was achieved between the measurement and modelling result.

The influence of the damaged paint effect was investigated. The paint status is assumed as the same as the design phase. The anode currents at the different ship velocities are illustrated in figure 6.

5 Conclusions

Optimization design of ICCP system of ship with complicated structure was realized using boundary element technology combining with optimization algorithm. As the result, an evenly distributed protection potential is achieved. The ICCP system was evaluated while ship is travelling in different speeds and paint status.

Reference

1. R. Verbeek, Riva-Lips., Application of Waterjet in High-Speed Craft, Development in Marine Technology, 10, Hydrodynamics: Computations, Model Tests and Reality, Elsevier Press, 1992
2. DeGiorgi, V. E., Luas, K.E., Thomas, E. D. and Shimko, M. J., Boundary Element Evaluation of ICCP System under Simulated Service Conditions, Boundary Element Technology VII, 1992
3. Zamani, N. G., Porter, J. F. and Mufti, A. A., A Survey of Computational Efforts in the Field of Corrosion Engineering, Int. J. Numerical Methods in Engrg., Vol. 23, 1986
4. Adey, R. A., Niku, S. M., Computer Modelling of Corrosion using the Boundary Element Method, Computer Modelling in Corrosion, ASTM STP-1154, 1992
5. R. A. Abey and Pei Yuan Hang, Computer Simulation as an Aid to Corrosion Control and Reduction, NACE, Conference 99, San Antonio, Texas, USA, Apr., 1999
6. Brebbia, C. A. Boundary Element Method for Engineerings, Pentech Press, 1980
7. Strommen, R. S. Computer Modelling of Offshore Cathodic Protection Systems: Method and Experience, Computer Modelling in Corrosion. ASTM STP 1154, Philadelphia, 1992
8. Harvey P. Hack, Atlas of Polarisation Diagrams for Naval Materials in Seawater. Carderock Division, Naval Surface Warfare Centre, Apr. 1995
9. H. Kaesche, Metallic Corrosion, National Association of Corrosion Engineerings, Houston, Texas, 1985
10. H. G. Wrangler, J. Berendson and G. Karlberg, Physicochemical Hydrodynamics, D. B. Spalding, ed., Billing & Sons, Ltd., London, 1977
11. J. E. Plapp, Engineering Fluid Mechanics, Prentice-Hall, New Jersey, 1986
12. Computational Mechanics, BEASY-CP User Guide, Computational Mechanics BEASY, Aug. 1996
13. DeGiorgi, V. E., Finite Resistivity and Shipboard Corrosion Prevention System Performance, Boundary Element Technology XIII, 1997
14. R. Fletcher, Practical Methods of Optimization, Chichester, UK, Wiley, 1980